To be submitted for publication

LBL-8826 C.2
Preprint

FLAME ADVECTION AND PROPAGATION ALGORITHMS

Alexandre Joel Chorin

February 1978

Prepared for the U. S. Department of Energy
under Contract W-7405-ENG-48

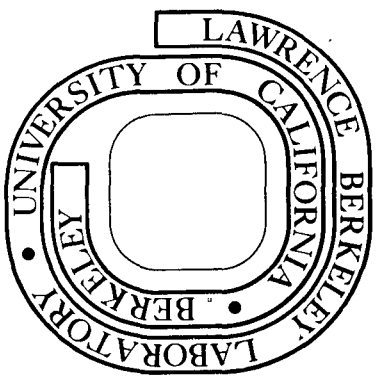

DISCLAIMER

LBL-8826

FLAME ADVECTION AND PROPAGATION ALGORITHMS*

Alexandre Joel Chorin

Department of Mathematics and Lawrence Berkeley Laboratory
University of California, Berkeley, California 94720

*Partially supported by the Engineering, Mathematical, and Geosciences Division of the U.S. Department of Energy under contract W-7405-ENG-48, and by the Office of Naval Research under contract N00014-76-0-0316.

FLAME ADVECTION AND PROPAGATION ALGORITHMS

Alexandre Joel Chorin

ABSTRACT

We present a simple algorithm for approximating the motion of a thin flame front of arbitrary shape and variable connectivity, which is advected by a fluid and which moves with respect to the fluid in the direction of its own normal. As an application, we examine the wrinkling of a flame front by a periodic array of vortex structures.

Outline of goal and method

Consider a fluid occupying a domain D with boundary ∂D, in two or three dimensional space. The fluid in a subdomain $D_1 \subset D$ is burned, the fluid in $D_2 = D - D_1$ is unburned, and the boundary ∂D_1 between D_1 and D_2 is transported by the velocity of the fluid and also moves with a velocity U in the direction of its own normal; D_1 is expanding while D_2 is contracting. U is the flame speed, and may depend on such parameters as the temperature of the fluid, its chemical composition, or the distance from a solid wall. D_1 and D_2 are not assumed to be connected or simply connected. The need to represent the motion of the interface between D_1 and D_2 arises in a number of combustion problems; for example, in a number of applications one can consider a flame front as a discontinuity which acts as a source of specific volume, and the induced velocity field can be computed if the location of the flame can be found accurately.

By analogy with shock dynamics, one may attempt either to follow flames explicitly as hydrodynamic discontinuities, or one may hope to have a hydrodynamical calculation locate the flames by solving the appropriate equations without any explicit allowance for the presence of a flame. The former course runs into difficulty because normals are difficult to find in a manner which is both stable and accurate, and because programming can be overwhelmingly complex in situations where flames form pockets, reconnect, etc. The latter course runs into difficulty because flame velocity, unlike shock velocity, is not determined by the basic conservation laws (see, e.g., [6],[7]) and its determination as an intrinsic part of a general

program requires an accurate and expensive evaluation of chemical reaction and heat transfer rates.

In the present paper we present an alternative to both of these courses, through the use of a Huyghens principle. For the sake of simplicity, we consider a situation in which U is a constant throughout the fluid. (The case of variable U is not essentially different.) Let D_1 be the expanding region containing burned gas. Let $\underline{u}_1,\underline{u}_2,\ldots,\underline{u}_n$ be a collection of vectors, with magnitudes $|\underline{u}_i| = U$, $i = 1,\ldots,n$, and whose directions are equidistributed on the unit sphere (or the unit circle in the case of plane flow). Consider the regions $D_1^{(1)},D_1^{(2)},\ldots,D_1^{(n)}$ obtained from D_1 by rigid translations with translation vectors respectively $\underline{u}_1k,\underline{u}_2k,\ldots,\underline{u}_nk$, where k is a time step. The union of the $D_1^{(\ell)}$, $\bigcup_{\ell=0}^{n} D_1^{(\ell)}$, $(D_1^{(0)} = D_1)$ approximates, for n large enough, the body obtained from D_1 by having the boundary of D_1 move with velocity U in the direction of its normal during the time interval k. This construction is an implementation of the classical Huyghens principle: If one takes points on the boundary of D_1, starts spherical flames expanding with velocity U from each one of the points, and then constructs the union of the volume D_1 and the volumes covered by these spherical flames, the resulting body is identical to $\cup D_1^{(\ell)}$.

The construction above requires an algorithm for performing rigid body translations and can in fact be based on any such algorithm. In the applications we have carried out, we found it convenient to use a translation algorithm based on the simple line interface advection algorithm (Noh and Woodward [14]). We shall explain this algorithm in the next section. In the following section we shall use this algorithm to implement the Huyghens

principle and demonstrate that the accuracy of the resulting propagation algorithm is higher than that of the underlying advection algorithm. In a final section, we shall apply a combined advection/propagation algorithm to the analysis of the effect of intermittency on the velocity of a wrinkled thin flame in a model flow.

A simple line advection algorithm

Consider a grid with mesh length h superposed on a domain D. For simplicity, we assume D is two dimensional. The centers of the mesh cells are located at $x = ih$, $y = jh$, i,j integers (figure 1). A velocity field is given on the associated staggered grid (Harlow and Welch [11]); the horizontal velocity $u_{i+\frac{1}{2},j}$ is given at the centers $([i+\frac{1}{2}]h,jh)$ of the vertical sides of the cells, and the vertical velocity $v_{i,j+\frac{1}{2}}$ is given at the centers $(ih,[j+\frac{1}{2}]h)$ of the horizontal sides. Each cell in the grid may contain burned as well as unburned fluid, and the volume fraction f_{ij} of burned fluid is given in each cell; $0 \leqslant f_{ij} \leqslant 1$. To clarify the discussion, we shall call burned fluid "black" and unburned fluid "white". The task at hand is to transport the black fluid through D with the given velocity field $\underline{u} = (u,v)$. This can be done only if the interface between black and white volumes can be reconstructed from the given partial volumes f_{ij}.

The ideas in the simple line interface algorithm (Noh and Woodward [14]) are as follows: An interface is drawn in each cell on the basis of

an inspection of the partial volumes f_{ij} in the cell itself and in its immediate neighbors; the interface consists of horizontal and vertical lines and is made as simple as possible. The velocity at the interface is then produced from the given velocities by interpolation (in our program, by linear interpolation). The black volume is transported in two fractional steps, one vertical and one horizontal; the geometry of the interfaces is adapted to the direction of the flow, and it is not required that the interface constructed for the horizontal half-step coincide with the interface constructed for the vertical half-step.

Consider the horizontal half-step, and consider a cell centered at (ih,jh) with partial volume f_{ij}. We distinguish the following cases:

I. (no interface). $f_{ij} = 0$ or $f_{ij} = 1$. This is the simplest and usually by far the most frequent case. The fluid in the cell moves as a whole, with the right side moving with velocity $u_{i+\frac{1}{2},j}$ and the left side with velocity $u_{i-\frac{1}{2},j}$. With appropriate programming, usually nothing is actually computed in this case.

II. (vertical interface). $0<f_{ij}<1, f_{i+1,j}=0$ and either $f_{i,j+1}=0$, $f_{i,j-1}=0$ or $f_{i,j+1}>0, f_{i,j-1}>0$. It is reasonable to guess that the interface is vertical and located at $x = (i-\frac{1}{2})h + f_{ij}h$ (figure 2a). The following three cases are identical, except for an interchange of the roles of right and left and/or the roles of black and white:

a. $0 < f_{ij} < 1$, $f_{i-1,j} = 0$, $f_{i+1,j} > 0$, with either $f_{i,j+1} = f_{i,j-1} = 0$ or $f_{i,j+1} > 0$, $f_{i,j-1} > 0$;

b. $0 < f_{ij} < 1$, $f_{i-1,j} < 1$, $f_{i+1,j} = 1$, with either $f_{i,j+1} = f_{i,j-1} = 1$ or $f_{i,j+1} < 1$, $f_{i,j-1} < 1$;

c. $0<f_{ij}<1$, $f_{i-1,j}=1$, $f_{i+1,j}<1$, with either $f_{i,j+1}=f_{i,j-1}=1$ or $f_{i,j+1}<1$, $f_{i,j-1}<1$.

III. (horizontal interface). $0<f_{ij}<1$, $0<f_{i+1,j}<1$, $0<f_{i-1,j}<1$. The cell is assumed to contain a horizontal interface located at $y = (j-\frac{1}{2})h + f_{ij}h$ (figure 2b).

IV. (corner). $0 < f_{ij} < 1$, $0 < f_{i-1} < 1$, $f_{i+1,j} = 0$, $f_{i,j+1} = 0$, $f_{i,j-1} > 0$ (figure 2c). The black fluid is assumed to lie in a rectangle in the lower left corner of the cell; the horizontal side of the rectangle has length a, and the vertical side has length b. We must have

$$ab = f_{i,j} .$$

We also require

$$\frac{b}{a} = \frac{f_{i,j-1}}{f_{i,j}} ,$$

whenever this equation leads to $b \leqslant h$, $a \leqslant h$. If this equation leads to $b > h$, we set $b = h$ and $a = f_{ij}/h$; if this equation leads to $a > h$ we set $a = h$ and $b = f_{ij}/h$. There are seven related cases, three of which yield black rectangles in one of the other three corners, and each of the remaining four leads to a white rectangle in one of the corners. These are obtained by appropriate interchanges of the roles of top and bottom, right and left, and black and white.

V. (thin finger). $0 < f_{ij} < 1$, $f_{i+1,j} = f_{i-1,j} = 0$. The black fluid is assumed to occupy a thin finger inside the cell (figure 2d). The exact location of the finger is chosen at random as follows: The black finger

occupies the region $a \leq x \leq b$, $a = (i-\frac{1}{2})h + \frac{1}{2}(1-f_{ij})\theta$, $b = a + f_{ij}$, where θ is a member of a sequence equidistributed on $[0,1]$. Examples of suitable equidistributed sequences can be found in Lax [13], Chorin [4], Colella [8]. At each time half step, a new θ is chosen, but for a fixed time, the same θ is used in all cells in which this case occurs. A related case is found by exchanging the role of black and white.

The constructions in cases I, II, III were used in Noh and Woodward [14]. Their work contains additional features designed to describe effectively the motion of a fluid system with many components. Case IV is introduced here to improve the resolution of the method. Case V is important because in our application it occurs often. In [14], the finger is placed in the middle of the cell, and as a result the displacement of the finger is determined by the Courant number uk/h rather than by the velocity u (this remark is due to C. Fenimore [9]). The remedy proposed here is based on the Glimm construction ([10],[4]), and it ensures that on the average the motion of the finger is computed correctly. Fenimore [9] has proposed a more accurate remedy. It is known from experience with other random choice methods that the numbers θ_1 and θ_2 used in the horizontal and vertical half-steps must be independent. In the calculations to be described, we follow Colella and use two independent van der Corput sequences for the θ's.

The algorithm is stable whenever the Courant condition $(\max|u|)k/h < \frac{1}{2}$ is satisfied.

As an example, consider a rectangle of black fluid occupying 21 cells, transported by a "fluid" undergoing rigid body rotation centered at 0. The distance of the center of the rectangle from 0 is five cells (the problem

can be scaled independently of h). In figure 3 we display on the right the original configuration of the black fluid, and on the left the computed configuration obtained after a rotation of 180°. The lines are drawn as they are interpreted by the program. The uncertainty in the position of an interface is always less than one mesh length and, as can be expected, is largest at the corners. The accuracy is competitive with that of other methods for performing advection calculations.

Implementation of the Huyghens principle

Consider a region $D_1 \subset D$ in the plane whose boundary is propagating with velocity U. At time $t = nk$, n integer, D_1 is described by an array of partial volumes, f_{ij}^n. Consider the 8 angles $\alpha_\ell = (\ell-1)\pi/4$, $\ell = 1,\ldots,8$, and the corresponding translation vectors $\underline{u}_\ell = (U \cos \alpha_\ell, U \sin \alpha_\ell)$. Use the algorithm described in the previous section to translate the area (described by the f_{ij}) successively by each one of the velocity fields u_ℓ; this results in 8 new areas $f_{ij}^{(\ell)}$, $\ell = 1,\ldots,8$. Write $f_{ij}^{(0)} = f_{ij}$, and then write

$$f_{ij}^{n+1} = \max_{0 \leqslant \ell \leqslant 8} f_{ij}^{(\ell)} .$$

This is our implementation of the Huyghens principle.

Note the following facts:

(i) Each cell in the grid has 8 neighbors. The amount of mass transported from any one cell to any one of its neighbors is largest when the translation vector points from the center of the given cell to the center of the neighboring cell. All such directions coincide with one of the directions determined by the α_ℓ. Any additional directions are redundant and will not affect f_{ij}^{n+1}.

(ii) In three dimensional space, 26 directions are needed. The amount of resulting labor is still modest if care is taken to ensure that the calculations are performed only when they are needed, i.e., when $0 < f_{ij} < 1$ in a cell under consideration or in a neighboring cell.

(iii) In the plane a single pair of θ's in case V is sufficient for all translations during a given time step; a single triplet is needed in three dimensions.

(iv) Alternate strategies for implementing the Huyghens principle, in which fewer directions are used in conjunction with a sampling strategy for the angles, have been tried, but resulted in modest savings in computing effort with a non-negligible loss in accuracy.

The accuracy of the propagation algorithm just described was consistently higher than that of the underlying advection algorithm in all cases we ran. There are two explanations: (i) the advection algorithms are most accurate when the velocity field is one dimensional, which is the case in each one of the translations used to implement the Huyghens principle, and

(ii) if the propagation algorithm underestimates or overestimates the length of the interface, the error is self-correcting to a substantial extent. As an example, we ignited the fluid in one fluid cell and followed the resulting flame propagation; in figure 4 we display the flame front obtained with $U = 0.2$, at $t = 1.83 = 70k$, $h = 1/19$, $Uk/h = .099$. The fractional volumes at the edge of the flames are drawn as they are interpreted by the program. The slight asymmetry reflects the effect of the θ's. The middle square is the square ignited at $t = 0$.

The original area of burned fluid is h^2, which equals the area of a circle of radius $r_o = h/\sqrt{\pi}$. The area of burned gas should be approximately $A = \pi(r_o + Ut)^2$. Let A_c be the area of burned gas as computed by the program, $A_c = \Sigma f_{ij} h^2$. In table I we display the area A_c, the error $A - A_c$, and the relative error $(A - A_c)/A_c$, with the parameters h, U, Uk/h, as above. Note that for small $t = nk$, substantial contributions to the value of $A - A_c$ are due to the fact that our formula for A is not exact, as well as to the statistical fluctuations in A_c due to the reliance on the θ's. The algorithm does perform well.

If the flame is advected by a fluid while it is propagating, the advection algorithm and the propagation algorithm can be used as successive fractional steps in the determination of the location of the front. The propagation algorithm is stable whenever the underlying advection algorithm is stable.

TABLE I

Error in a circular flame calculation, h = 1/19

n	A_c	$A_c - A$	$(A_c - A)/A_c$
1	.0038	-.000039	-.010
2	.0049	.000093	.018
5	.0091	.00064	.065
10	.019	.0011	.054
20	.056	.00080	.014
30	.110	-.00028	-.0025
40	.181	-.0013	-.0070
50	.269	-.0028	-.0085
60	.386	-.0033	-.0086
70	.497	-.0038	-.0077
80	.636	-.0044	-.0069

The effect of intermittency on the velocity of wrinkled flames

We now present an application of the method above to a simplified problem in flame theory. (An excellent account of the subject can be found in Williams [17].) Under conditions which are often encountered in practice, one believes that a turbulent flame propagates faster than a laminar flame mainly because a turbulent velocity field wrinkles the flame and increases the area available for burning. Let the velocity of the turbulent flame be denoted by u_a, and let $u_\ell \equiv U$ be the velocity of an unwrinkled flame in a fluid of the same temperature and composition. It has been observed from experiments (Andrews et al. [1]) that in many situations the ratio u_a/u_ℓ is roughly proportional to the intrinsic Reynolds number $R_\lambda = u'\lambda/\nu$, where u' is the r.m.s. intensity of the turbulence, λ is the Taylor microscale (for a definition, see e.g. [15], [1]), and ν is the viscosity. According to recent theories, turbulence can be usefully described as a random array of vortices [see e.g. [4]). A theory described in [3] and experiments described in [12] lead one to believe that these vortices are rod-like, and thus a two-dimensional calculation, performed in a plane normal to the axes of these vortices, should describe their main effects. A calculation presented by Tennekes [15] suggests that λ is the order of magnitude of the diameter of these vortices.

Thus, in order to provide the simplest possible explanation of the observation of Andrews et al., we are led to the following problem: Consider a time-independent periodic array of vortical structures in the plane. At $t = 0$ a plane flame front coincides with the y axis. We

wish to follow the wrinkling of the flame front and the consequent increase in the velocity of the flame.

The velocity field is periodic with period $L = 1$ in both x and y directions. Consider one periodic box, $-\frac{1}{2} \leq x \leq \frac{1}{2}$, $-\frac{1}{2} \leq y \leq \frac{1}{2}$. Consider the velocity field given by $\underline{u} = (u,v)$, $u = -\partial_y \psi$, $v = \partial_x \psi$, where $\psi = C \exp(-(x^2+y^2)/\lambda^2)$. λ is the "microscale". $\underline{u}$ is not periodic, and although it does satisfy the equation $\operatorname{div} \underline{u} = 0$, it does not satisfy the discrete equations $D\underline{u} \equiv u_{i+\frac{1}{2},j} - u_{i-\frac{1}{2},j} + v_{i,j+\frac{1}{2}} - v_{i,j-\frac{1}{2}} = 0$. $D\underline{u} = 0$ guarantees that the area occupied by burned gas increases only due to burning (except for possible small errors due to the interpolations used in the advection algorithm). The component of $\underline{u}$ which is periodic and satisfies the equations $D\underline{u} = 0$ is obtained by the projection algorithm described in [2]. The constant C is then adjusted so that

$$u' = \sqrt{\sum_{\text{box}} (u^2+v^2)h^2} = 1 .$$

In figure 5 we display a typical flow configuration in a periodic box. At $t = 0$, the flame coincided with the left wall of the box. The front is shown at $t = 1.53$, $n = 125$, with $u_\ell = 0.2$, $\lambda = 0.2$, $h = 1/19$. The partial volumes are drawn as they are interpreted in a horizontal sweep, and occasional ambiguities are removed by diagonal lines.

The viscosity ν does not appear explicitly in our model; indeed, ν governs the rate at which vortical structures appear and disappear, and in our problem they do neither.

Let $A(t)$ be the portion of the periodic box occupied by burned fluid. Define $u_a = dA/dt$. Simple scaling arguments show that u_a/u_ℓ can be a

function of the ratios $u'u_\ell = 1/u_\ell$ and $\lambda/L = \lambda$ only. Thus the analogue of the law of Andrews et al. is

$$\frac{u_a}{u_\ell} = \text{constant} \times \frac{u'}{u_\ell} \frac{\lambda}{L} = \text{constant} \times \frac{\lambda}{u_\ell} .$$

However, the original law $u_a/u_\ell \sim u'\lambda/\nu$ and the new law $u_a/u_\ell \sim \lambda/u_\ell$ are essentially different, since the latter implies that $u_a \sim \lambda$ independently of u_ℓ. This last conclusion is untenable and disappears only if it can be shown that u_a/u_ℓ is roughly independent of u'/u_ℓ. For $u' \gg u_\ell$, this last statement is indeed true. In figure 6 we display u_a/u_ℓ as a function of the appropriately scaled time $t^* = tu_\ell/0.2$ for several values of u_ℓ. The curves coincide to a large extent, showing that u_ℓ does not affect greatly the generation of new surface by vortical motion.

It is clear that if u_a/u_ℓ is roughly independent of u'/u_ℓ, the generation of new surface is roughly proportional to the scale λ of the vortical structures. In figure 7 we display the variation of u_a/u_ℓ with λ as a function of time. It can be seen that for a given t the value of u_a/u_ℓ is indeed roughly proportional to λ. u_a/u_ℓ increases when the vortex meets the flame, then decreases when the flame consumes the newly added flame length. The calculation was stopped when the flame was overflowing the box. Thus, in the narrow confines of our model problem, we have a reasonable explanation of the observation offered in [1].

Acknowledgment

I would like to thank Mr. William Noh for helpful discussions and for introducing me to the simple line algorithm.

Bibliography

[1] A. E. Andrews, D. Bradley, and S. Lwakabamba, Combustion and Flame, 24, 285 (1975).

[2] A. J. Chorin, Math. Comp., 22, 745 (1968).

[3] A. J. Chorin, Proc. 2nd Int. Conf. Num. Meth. Fluid Mechanics, (1970).

[4] A. J. Chorin, J. Fluid Mech., 63, 21 (1974).

[5] A. J. Chorin, J. Comp. Phys., 25, 253 (1977).

[6] A. J. Chorin and J. E. Marsden, A Mathematical Introduction to Fluid Mechanics, Springer, New York (1979).

[7] R. Courant and K. O. Friedrichs, Supersonic Flow and Shock Waves, Interscience, New York (1948).

[8] P. Colella, Ph.D. thesis, University of California, Berkeley, Mathematics Department, 1979.

[9] C. Fenimore, private communication, 1978.

[10] J. Glimm, Comm. Pure Appl. Math., 18, 697 (1965).

[11] F. H. Harlow and J. E. Welch, Phys. Fluids, 8, 2182 (1965).

[12] A. Y. S. Kuo and S. Corrsin, J. Fluid Mech., 56, 447 (1972).

[13] P. D. Lax, SIAM Review, 11, 7 (1969).

[14] W. Noh and P. Woodward, Proc. 5th Int. Conf. Num. Meth. Fluid Mechanics, Springer, 1976.

[15] H. Tennekes, Phys. Fluids, 11, 669 (1968).

[16] H. Tennekes and J. L. Lumley, A First Course in Turbulence, MIT Press, Mass. and London (1972).

[17] F. A. Williams, Combustion Theory, Addison-Wesley. Reading, Mass. 1965.

List of figure captions

1. Computational grid for advection.

2. Cases considered in advection algorithm.

3. An example of advection.

4. Propagation of a circular flame.

5. Stretching of a flame by a vortical structure.

6. Effect of u_ℓ on u_a/u_ℓ.

7. Effect of scale on u_a/u_ℓ.

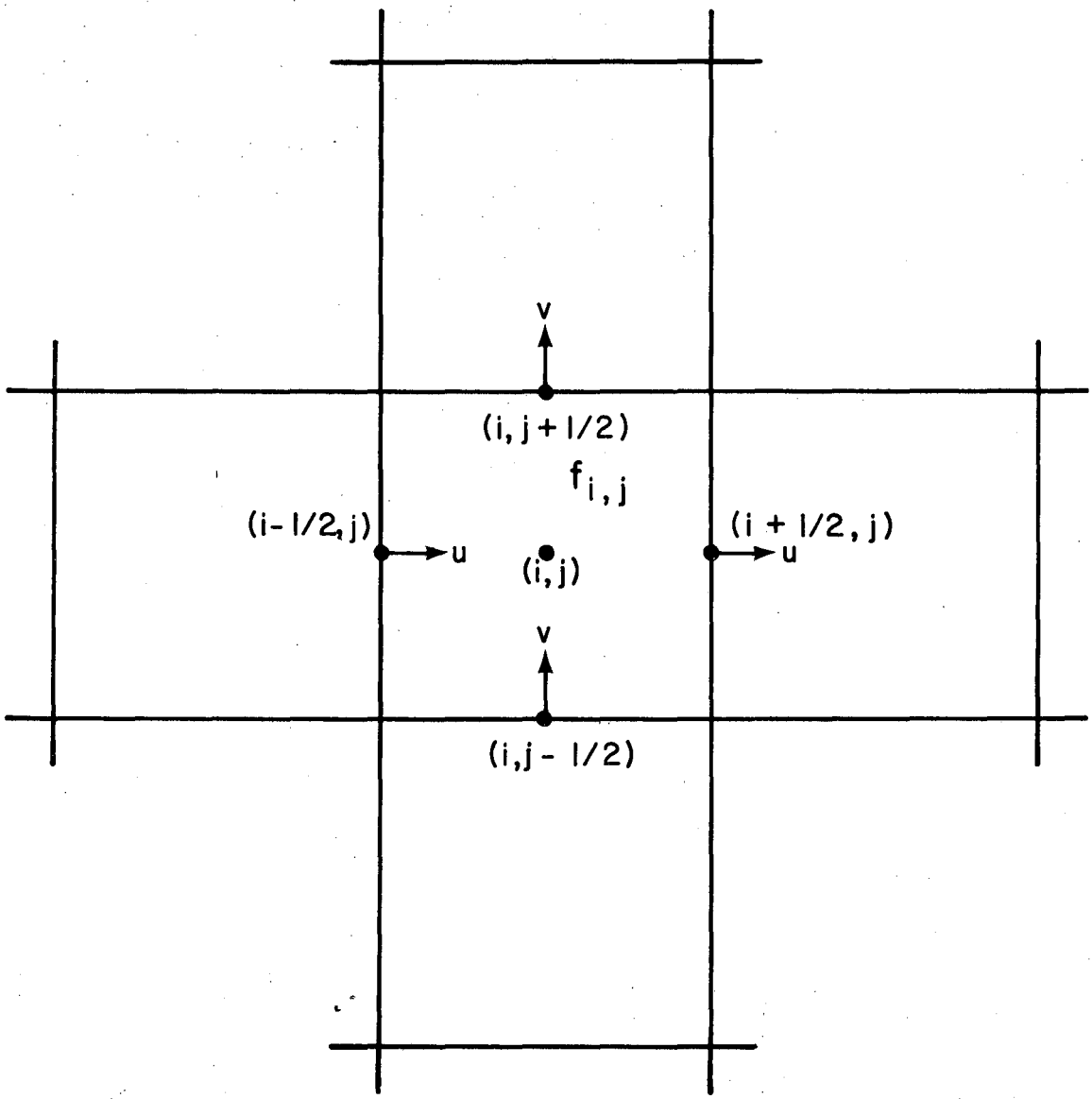

XBL 793-834

Figure 1

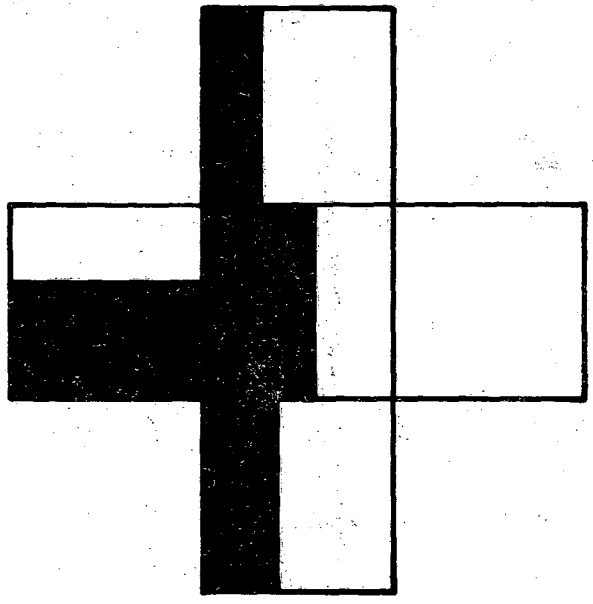

(a)

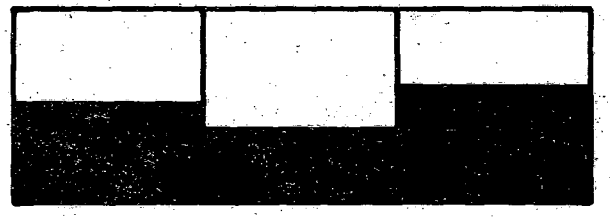

(b)

XBL 793-833

Figure 2(a) and Figure 2(b)

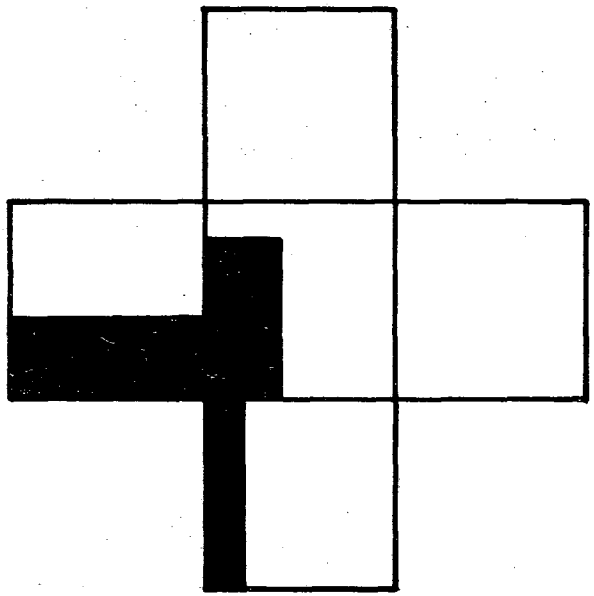

(c)

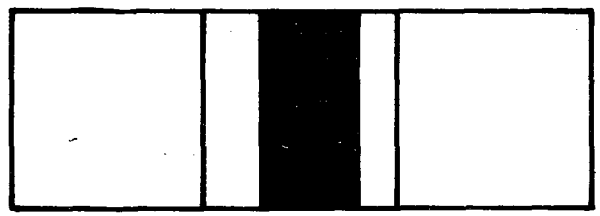

(d)

XBL 793-832

Figure 2(c) and Figure 2(d)

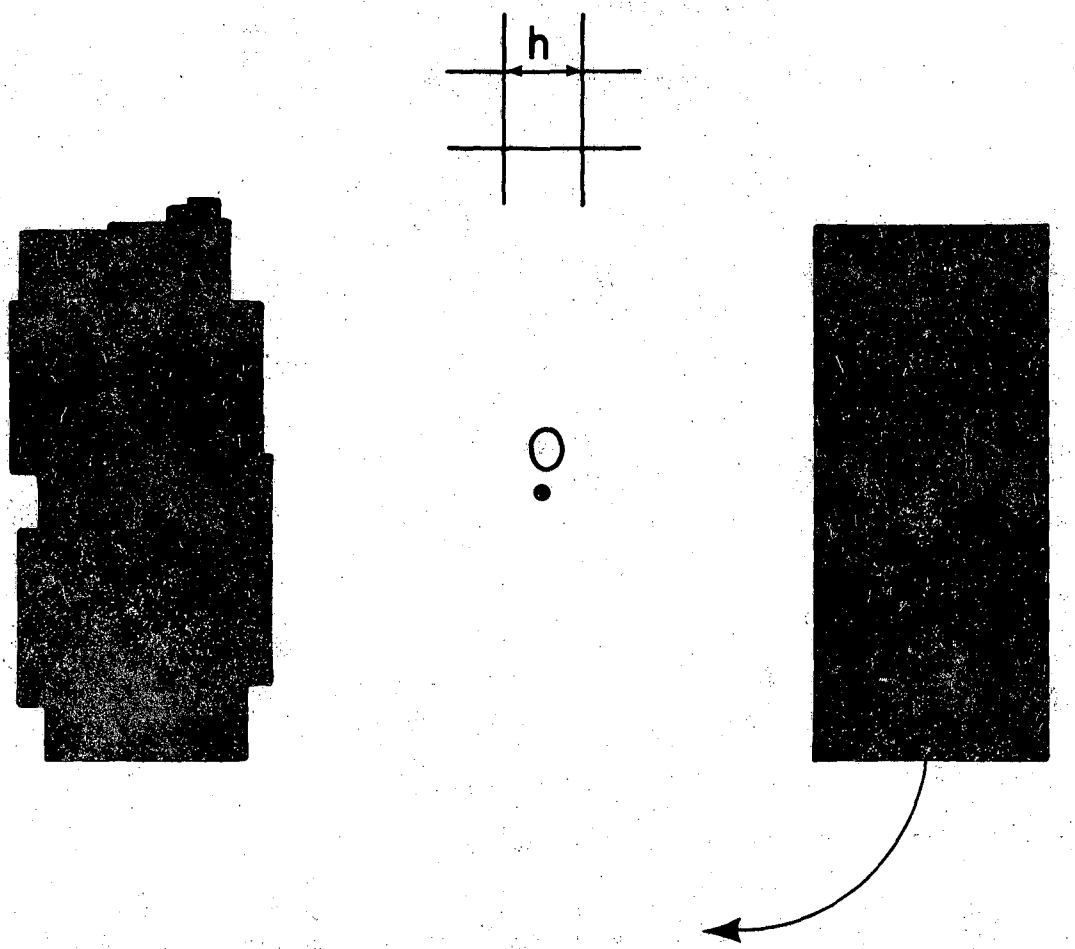

XBL 793-835

Figure 3

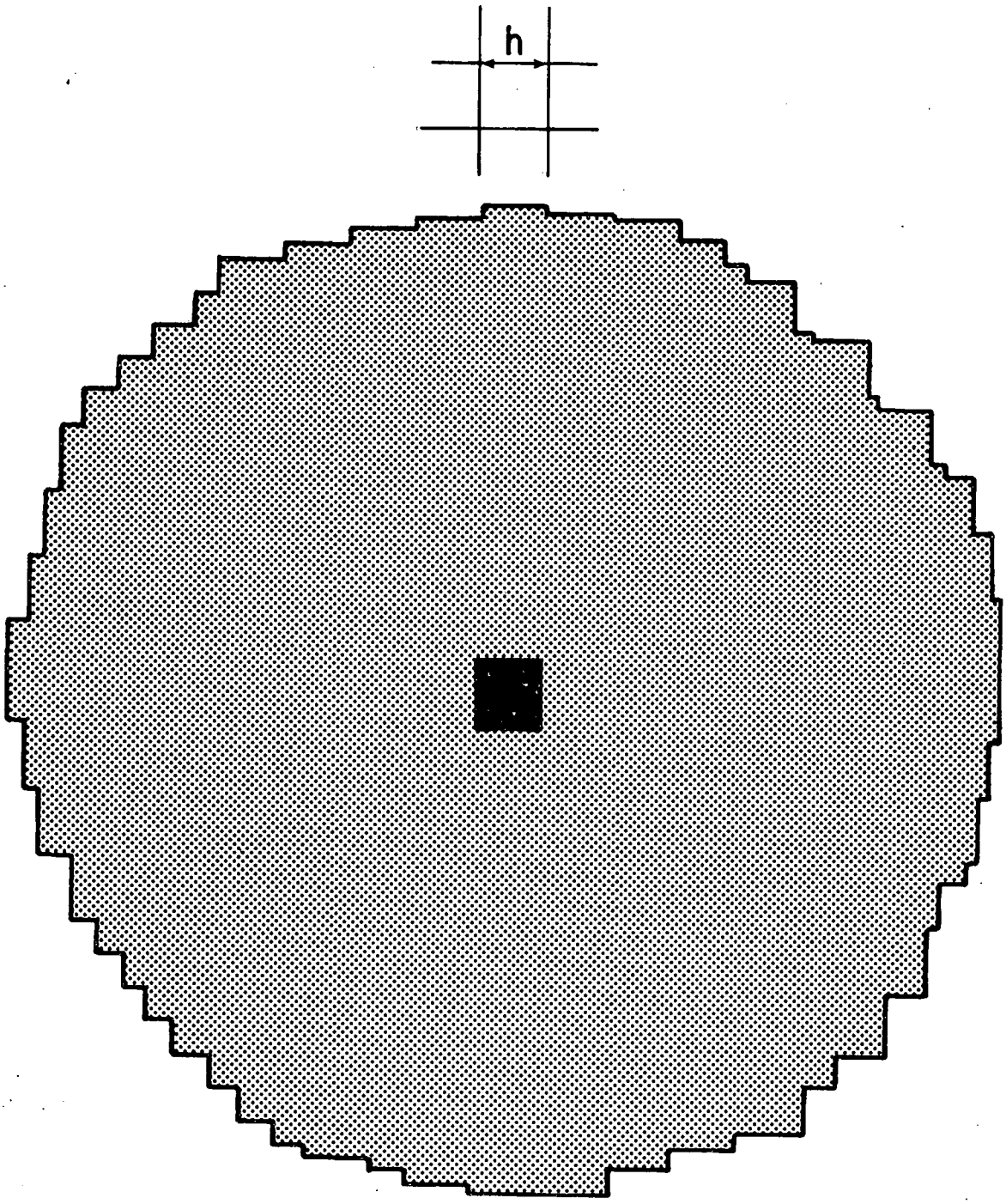

XBL 793-836

Figure 4

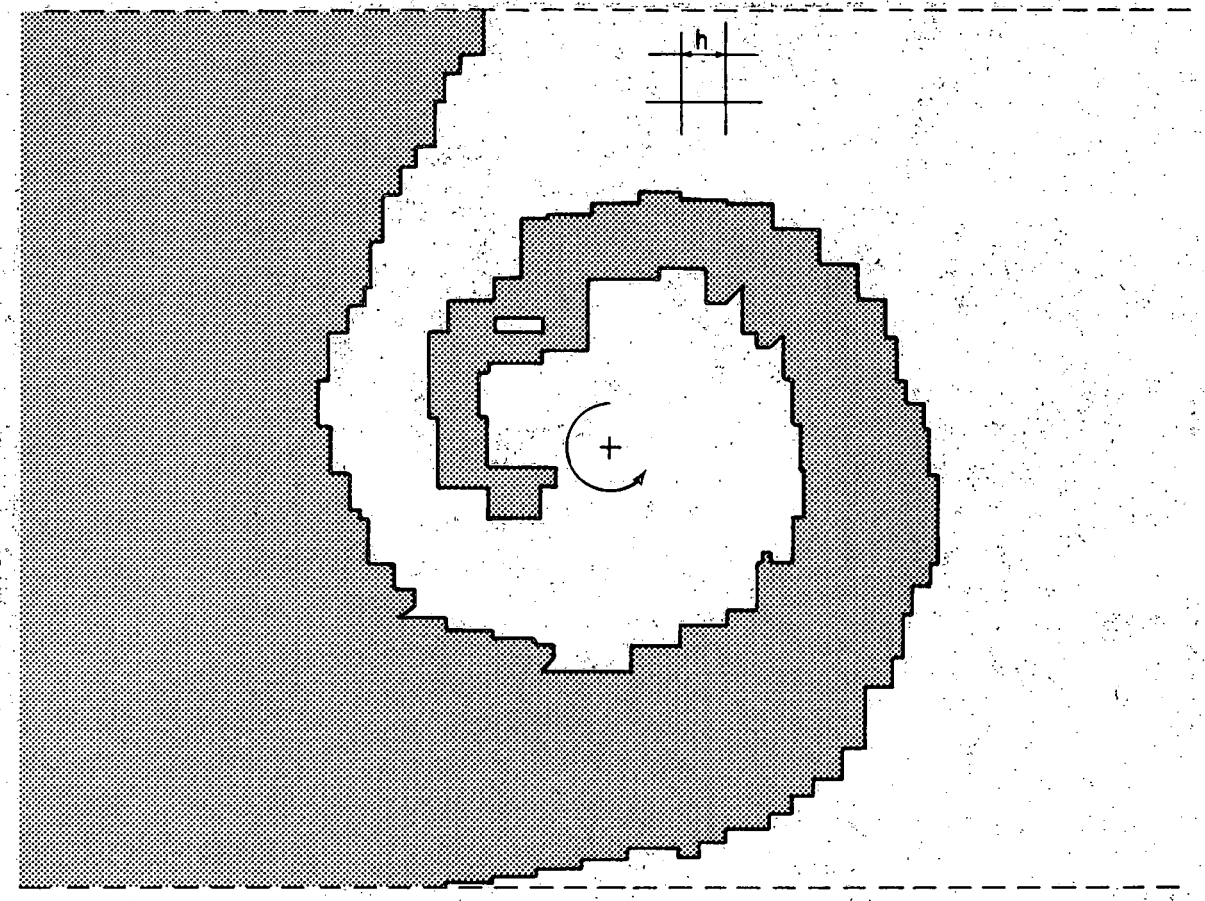

XBL 793-837

Figure 5

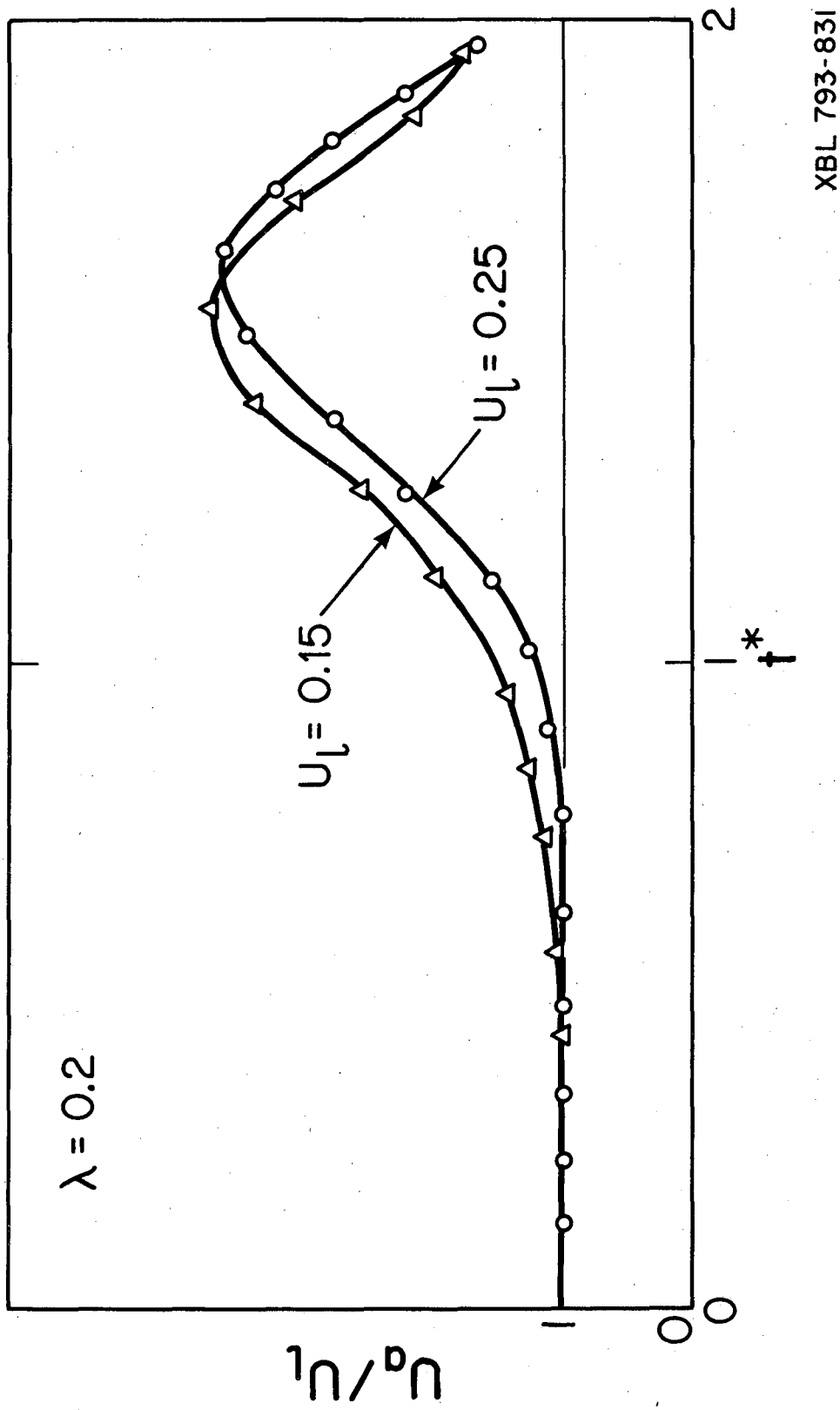

XBL 793-831

Figure 6

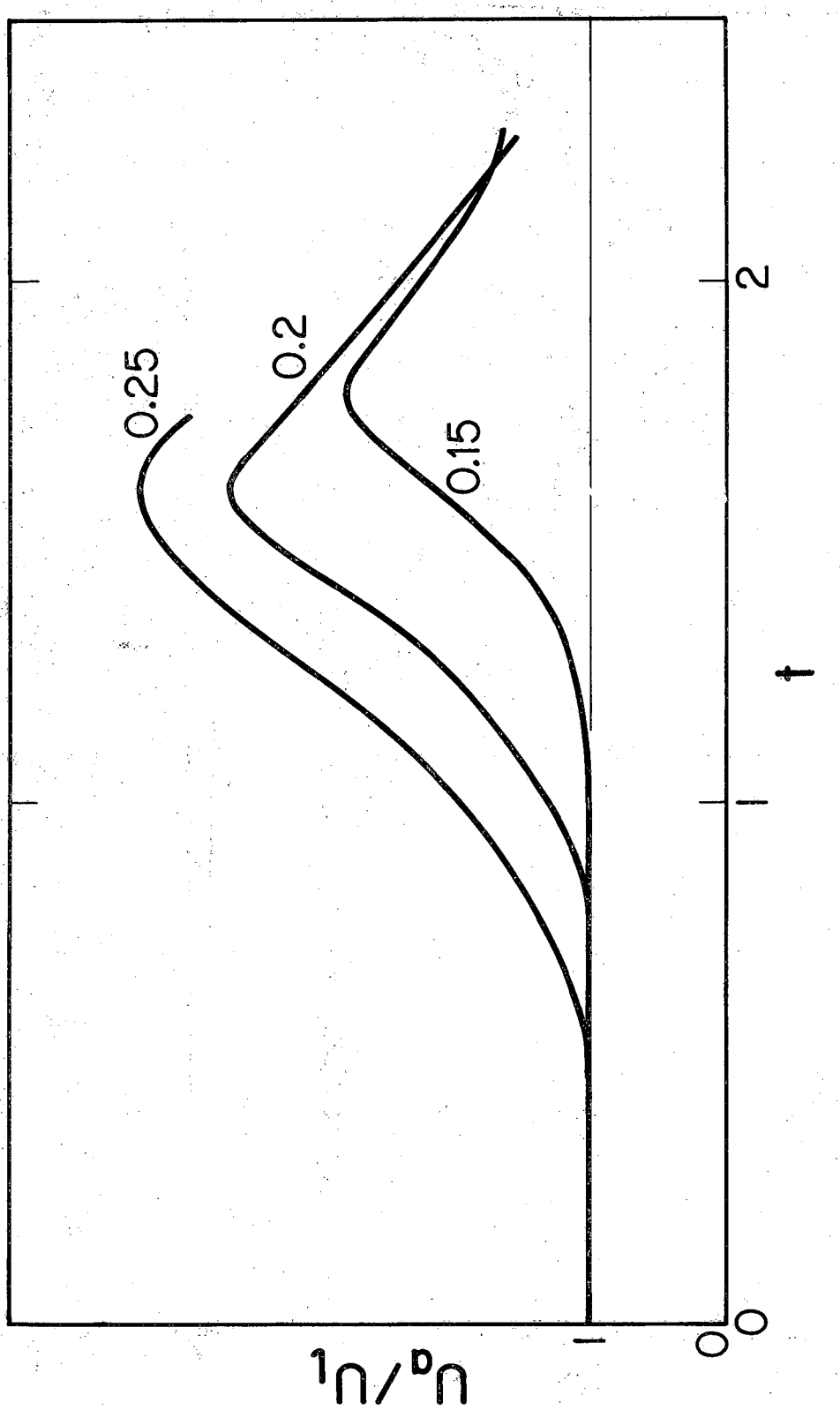

XBL 793-830

Figure 7

TECHNICAL INFORMATION DEPARTMENT
LAWRENCE BERKELEY LABORATORY
UNIVERSITY OF CALIFORNIA
BERKELEY, CALIFORNIA 94720